Full Length Research Paper

Using a gas-filled detector in a rotation modulation collimator system for near-field imaging

Tareq Alrefae

[1]Deptartment of Physics, Faculty of Science, Kuwait University, Khaldia, Kuwait.
[2]Center for Research in Environmental Radiation, Faculty of Science, Kuwait University, Khaldia, Kuwait.
E-mail: tareq.alrefae@ku.edu.kw. Tel: (+965) 24987780. Fax (+965) 24846498

Rotation modulation collimators (RMC) are a class of nuclear imaging devices that are found in various applications. RMC are used for far-field applications, as in astronomy, and in near-field applications, as in environmental, medical and military uses. The typical detectors used in RMC system are scintillators and semi-conductors, which detect γ radiation only. This work investigates the utilization of gas-filled detectors, which detect β particles as well as γ rays. Hence, a simple RMC system is built that utilizes a Geiger-Muller (GM) tube as a detector. To help assess the new system, a direct image construction algorithm is developed. Results of the assessment show that the newly built system is well capable of imaging radiation sources in the near-field.

Key words: Rotation modulation collimators, mechanical collimators, nuclear imaging, Geiger-Muller (GM)-tube, time modulated imaging.
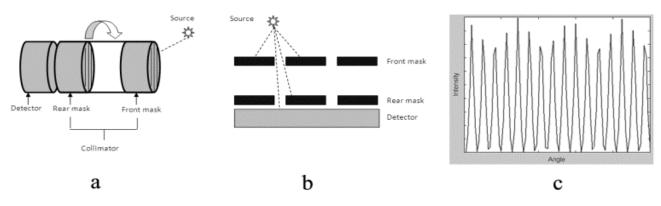
INTRODUCTION

Rotation modulation collimators (RMC) are a class of nuclear imaging apertures found in a wide range of applications. By spatially varying incoming signals, RMC produce planar images of distant and near γ radiation sources. Far-field RMC imaging is commonly employed in applications of astronomy (Smith et al., 2004). Near-field RMC imaging, on the other hand, is noticeably growing for medical, environmental and military applications (Sharma et al., 2008; Kowash et al., 2009; Kowash and Wehe, 2011).

A typical RMC consists of a detector that sits directly behind a pair of parallel, separated masks (Figure 1). Each mask is one dimensionally gridded by having photon-transparent regions (slits) and photon-opaque regions (slats). The masks rotate together about an axis perpendicular to the image plane. Depending on the angle of rotation, γ rays originating from the radiation source can make it to the detector by passing through slits of both masks. Alternatively, γ rays are stopped at slats of either mask, thus prevented from reaching the detector. This variation in detection gives rise to signal modulation that is a function of the angle of rotation (Figure 1c). With appropriate algorithms, this signal modulation is utilized to construct a planar image.

For image construction, algorithms with statistical features are commonly applied. The utilized statistics are compatible with the stochastic nature of the radioactive decay (Knoll, 2000). Such implementation often involves lengthy iterations to ensure convergence that leads to acceptable values, and thus correct image construction (Kowash et al., 2009).

A quick search in the literature reveals a number of successful prototypes of near field RMC imaging systems (Sharma et al., 2008; Kowash et al., 2009; Kowash and Wehe, 2011). Each prototype is unique in its field of application, algorithm of image construction, or hardware used. Typically, the types of detectors used in these prototypes are scintillators (Kowash et al., 2009; Kowash and Wehe, 2011) and semi-conductors (Sharma et al., 2008). This leaves the third type of detectors, namely, gas-filled, to be tested. A major difference between scintillators and semi-conductors on one hand and gas-filled detectors on the other hand, is that the latter are able to detect α, β and γ radiations, whereas the former can only detect γ radiation. Hence, the goal of this work is to assess the ability of gas-filled detectors in near field

Figure 1. An RMC system (a) is composed of a detector and two masks that rotate together. Depending on the angle of RMC rotation, γ rays may or may not reach the detector (b). Hence, the signal seen by the detector is a function of the RMC angle (c).

RMC imaging, taking into consideration detection of more than one type of radiation. To achieve this goal, a simple RMC prototype is built that mainly consists of a Geiger-Muller (GM) tube serving as a detector. Moreover, a straightforward image construction algorithm is developed to assess the prototype's ability in locating radioactive sources.

MATERIALS AND METHODS

Hardware and apparatus

The basic components of the current RMC system are a GM tube serving as a detector and a pair of lead masks serving as an aperture. The 35 mm diameter GM tube is connected to a high voltage supply which in turn is connected to a PC. The GM tube is positioned right behind the rear mask. Each mask is placed in a holder that allows for manual rotation through 180°. Both holders are placed on an optical bench, thus allowing the masks to slide along a line that is perpendicular to the plane of the detector and the masks (Figure- 2). Each mask, essentially, has a diameter of 35 mm with 4 slits of 3 mm width. As for the image plane, it is resembled by a cardboard that is patterned with 10 mm square cells, with a 10 mm gap in between. Nine of these cells, that are arranged in a 3 × 3 matrix make up the field of view (FOV) (Figure 3).

A ^{137}Cs point source of 0.8 μ curie (Ci) activity is placed in a cell on the image plane for imaging. When it is desired to block β particles, a set of aluminium (Al) sheets are placed on a holder that is positioned between the image plane and the front mask. A total thickness of 4 mm is used for the Al sheets, such that the β particles with the highest energy ($E_{end\ point}$ = 1.176 MeV) are fully attenuated, while allowing the γ to freely pass (Knoll, 2000). Thus, two sets of data are gathered. One involves both β and γ radiation, in which the Al sheets are not used. The other set of data involves only γ radiation, in which the Al sheets are used to block out the β particles.

Image construction algorithm

The image construction algorithm is based on the uniqueness of signal modulation (*I*) to the location (r_0 , θ_0) of the radiation source on the image plane. This relation is evident in the equation (Smith et al., 2004; Sharma et al., 2008).

$$I(\theta_i) \sim r_0 \cos(\theta_i - \theta_0) \qquad (1)$$

where θ_i is the RMC rotation angle and *i* is a dummy variable that increments the RMC rotation angle from 0 to 180°. For example, a point source placed in cell 1 (Figure 3) would give a signal modulation that is quite different in its frequency and/or phase than if it were placed in any other cell. Thus, even for cells that are symmetric and have the same value of r_0, like cells 3 and 9, the difference in signal modulation arises from the argument of the cosine function, namely θ_i - θ_0, that varies with *i*.

With such a profound basis, the image construction algorithm executes two main steps. The first is constructing the transfer matrix (TM), which constitutes the modulated signal *I* (θ_i) as a function of the RMC angle for every cell in the image plane. The entries of the TM are organized as shown in Figure 4, where a set of values that are associated with a certain cell that make up a vector, known as the transfer vector (TV).

The construction of TM is initiated with manually placing a point source in the first cell. With both masks placed at an angle of θ = 0°, a reading is taken for a dwell time of *t*. Next, both masks are manually rotated to a new angle, thus incrementing the previous angle by Δθ. Then, a new reading is taken for the same dwell time duration. This procedure is repeated until the run of θ_i = 180° is completed. These runs give a set of data that form a TV of the first cell. To overcome statistical fluctuations, either the dwell time *t* is taken to be sufficiently long, or the readings are repeated a number of times before an average is calculated. The source is then manually placed in the next cell, and the same procedure is performed until the TM is completely constructed.

When the point source to be imaged is placed in a random, unknown cell, measurements are performed for all RMC angles for the same dwell time *t*, and the same increment Δθ. These measurements that correspond to this random, unknown cell give values that make up the measurement vector (MV), which has the same dimension as a TV. Ideally, the MV should be identical to one of the TVs that compose the TM, because of statistical fluctuations; however, a small difference arises.

The second main step that the algorithm executes is comparing the MV with all TVs that make up the TM. This comparison is done by performing subtraction operations of the MV and each TV. The operation that gives the least absolute value corresponds to the cell where the radiation is coming from. Hence, the unknown cell is revealed, and the image is constructed. The comparison operation is swiftly executed by a simply developed Matlab function that uses
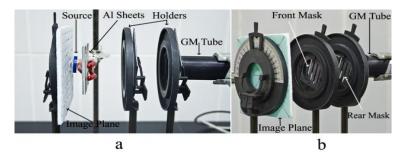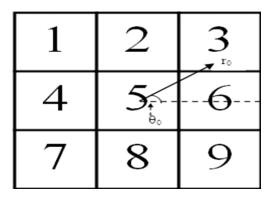
Figure 2. The apparatus.

Figure 3.   The FOV is made up of nine cells, where each cell has a label.
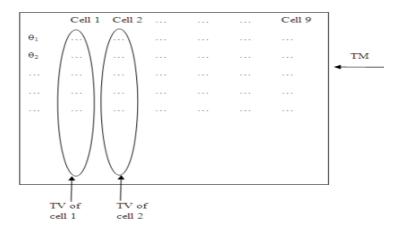

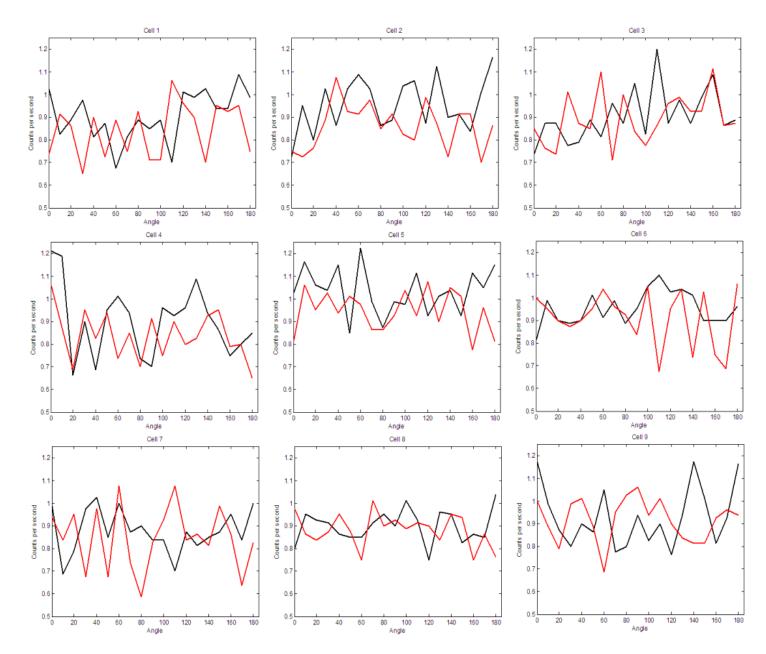**Figure 4.** The transfer matrix (TM) is composed of transfer vectors (TV).

TM and MV as input arguments.

RESULTS

The data gathered in this study fall in one of two categories. The first is of signals carrying β and γ radiation, while the other is of signals carrying γ radiation only. Consequently, the results are categorized accordingly.

Figure 5 shows modulation as a function of the RMC angle for $\beta + \gamma$ signals when the source is placed at nine different cells that make up the image lane. This figure also shows the modulation of the γ-only signals. The latter is obtained when the Al sheets are used to attenuate β particles, thus preventing it from reaching the

Figure 5. Modulation of β + γ signals (black), and γ-only signals (red) corresponding to each cell in the image FOV (t = 40 s.). Error bars are suppressed for clarity.
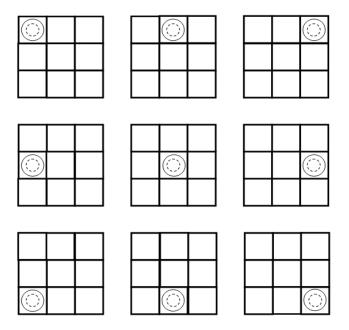
RMC, let alone the detector.

It is evident that both signals are modulated as functions of the RMC angle. This behavior is expected, since from Equation 1 some RMC angles allow more radiation to reach the detector, while others allow less for a given cell in the image plane. It is also evident that for a given cell, the β + γ signals are different in magnitude than the γ-only signals ($N_{\beta+\gamma}$ and N_{γ}, respectively). This difference is as shown in Table 1 where the ratio $N_{\beta+\gamma}$ / N_{γ} is presented. Clearly, $N_{\beta+\gamma}$ is greater than N_{γ} for all cells. This difference is easily understood since the former contains β as well as γ events, while the latter contains γ events only.

Figure 6 shows the output of the image construction algorithm. The solid and dotted circles in the figure represent actual and calculated locations, respectively of the source. Remarkably, the algorithm is able to correctly calculate the location for all nine cells, using either the β + γ signals or the γ-only signals. In other words, the presence of β particles in the signal does not hinder success in image construction, so long as the algorithm is properly developed and applied.

Table 1. The ratio of the total number of events of $\beta + \gamma$ signals and γ-only signals for all nine cells ($S = 15$ cm).

Cell	$N_{\beta+\gamma} / N_\gamma$
1	1.07512 ± 0.34563
2	1.10992 ± 0.35118
3	1.01028 ± 0.33504
4	1.07535 ± 0.34566
5	1.09318 ± 0.34852
6	1.04769 ± 0.34119
7	1.03416 ± 0.33898
8	1.0194 ± 0.33655
9	1.01435 ± 0.33572

Figure 6. FOV in nine different cases. In each case, the solid circle represents the actual point source location, whereas the dotted circle represents the location as calculated by the algorithm. The algorithm is successfully able to find the desired locations, thus both circles coincide in all cases. The success of the algorithm is observed using $\beta + \gamma$ signals and γ-only signals.

DISCUSSION

The aim of this study is to test the imaging ability of gas-filled detectors in near fried RMC applications. Unlike scintillators and semi-conductors which detect γ radiation only, gas-filled detectors are able to detect α, β and γ radiation. Because α particles are short-ranged in non-vacuum environments, it will not reach the detector when air separates the detector from the source, unless they are very close. β particles on the other hand may or may not reach the detector. Evidently, if the separation

distance between the detector and the source (S) is long, as in the far-field applications, β particles will not reach the detector (Knoll, 2000). If S is short, however, as in the near-field applications, β particles can make it to the detector provided that their energies are sufficient (Knoll, 2000). As for γ radiation, its long-range feature allows it to reach the detector in spite of the length of S.

A gas-filled detector, thus, detects β and γ radiation when used in a near-field RMC system. This result is verified and observed in Figure 5. Nevertheless, the presence of β particles in the signal along with γ radiation does not restrict imaging abilities, provided that the image construction algorithm is appropriate. This result is evident in Figure 6, where the correct location of the source is calculated for every cell in the image plane, using both kinds of signals, namely with and with without β particles.

It should be noted, however, that the image construction algorithm used in this study is time consuming. For example, construction of a TM for a 3×3 image plane with $t = 40$ s., $\Delta\theta = 10°$ is roughly 2 h. Such a long time makes the algorithm impractical. Moreover, the 1×1 cm cell size makes the resolution too low. Nevertheless, the purpose of applying the algorithm is to demonstrate the ability of an RMC system with gas-filled detector to correctly locate the source albeit the presence of β particles in the detected signal. Improving or substituting the algorithm is left for future work.

The presence of β particles in the signal is caused by the radioactive decay of the point source. In this case, ^{137}Cs decays to ^{137m}Ba through a 0.514 MeV β-decay, before a 0.662 MeV γ ray is emitted, thus forming ^{137}Ba. Hence, this two-step process which constitutes around 94% of the ^{137}Cs decays, emits both, β and γ radiation. The remaining 6% or so decays are of a 1.174 MeV β-decays that transforms ^{137}Cs directly to ^{137}Ba without an intermediate metastable state (Knoll, 2000). Whether given off through a one-step or a two-step process, the β particle shares its energy with an anti-neutrino, which is a particle resulting from the β-decay. This sharing in energy does not give the β particle a certain energy value. Rather, a β particle may have any value of energy within a range, starting from zero up to a maximum of $E_{end\ point} = 1.174$ MeV. Therefore, β particles in the lower end of the range have insufficient energies, and thus will not be able to travel the separation distance S.

To travel a distance of 15 cm in air, a minimum energy of 0.15 MeV is needed for a β particle (Knoll, 2000). Interestingly, a glance at the β spectrum of ^{137}Cs reveals that almost one third of the β particles cannot travel an $S= 15$ cm (Knoll, 2000). Hence, the remaining two thirds may attempt to reach the detector. While some make it, others interact with the Pb mask and get attenuated. A portion of the β particles that interact with the Pb mask produce bremmstrahlung radiation, which are detected as γ rays provided that they travel in the right direction to

the detector. Therefore, β particles and γ radiation that are given off the ^{137}Cs source, along with the bremmstrahlung radiation, will sure enough make $N_{\beta+\gamma}$ greater than N_γ (Table 1). A theoretical model that quantitatively explains the interaction of β particles with the Pb masks is left for future work.

The limitations of this study can be brought to two main points. First, although using non-motorized apparatus give more flexibility, it may cause inaccuracies in the count values given by the GM tube. Second, the statistical nature of the GM tube introduces inaccuracies, which are remedied by taking relatively long measurements.

Conclusion

A near field RMC system that utilizes a gas-filled detector is presented. Unlike conventional RMC systems that detect γ rays only, this new system detects β particles, as well as γ rays. The system's ability to image is demonstrated using a newly developed image construction algorithm. Interestingly, it is shown that detection of β particles does not restrain the system's ability to correctly locate radiation sources in the near-field, and thus does not hinder its imaging ability.

The system is open for improvements in a number of ways. For example, motorization of the RMC and optimization of the image construction algorithm would certainly enhance the system's performance. These improvements are left for future work.

REFERENCES

Knoll GF (2000). Radiation detection and measurement. Wiley. New York.
Kowash BR, Wehe DK (2011). A unified near- and far-field imaging model for rotating modulation collimators. Nucl Instrum Meth A., 637: 178-184.
Kowash BR, Wehe DK, Fessler JA (2009). A rotating modulation imager for locating mid-range point sources. Nucl Instrum. Meth A., 602: 477-483.
Sharma AC, Turkington TG, Tourassi GD, Floyd CE (2008). Near-field high-energy spectroscopic gamma imaging using a rotation modulation collimator. Nucl. Instrum. Meth B., 266: 4938-4947.
Smith DM, Hurford GJ, Boggs SE (2004). Rotating modulation collimator imagers. New Astron. Rev., 48: 209-213.